Effect of the dynamic core-electron polarization of CO molecules on high-order harmonic generation

Cam-Tu Le,[1,2,*] Van-Hung Hoang,[3] Lan-Phuong Tran,[3] and Van-Hoang Le[1,3,†]

[1]*Atomic Molecular and Optical Physics Research Group, Advanced Institute of Materials Science, Ton Duc Thang University, 19 Nguyen Huu Tho Street, Tan Phong Ward, District 7, Ho Chi Minh City, Vietnam*

[2]*Faculty of Applied Sciences, Ton Duc Thang University, 19 Nguyen Huu Tho Street, Tan Phong Ward, District 7, Ho Chi Minh City, Vietnam*

[3]*Department of Physics, Ho Chi Minh City University of Education, 280 An Duong Vuong Street, District 5, Ho Chi Minh City, Vietnam*

(Received 28 February 2018; published 4 April 2018)

We theoretically investigate the influence of dynamic core-electron polarization (DCeP) of CO molecules on high-order harmonic generation (HHG) by solving the time-dependent Schrödinger equation (TDSE) within the single-active-electron (SAE) approximation. The effect of DCeP is shown to depend strongly on the molecular orientation angle θ. Particularly, compared to the calculations without DCeP, the inclusion of this effect gives rise to an enhancement of harmonic intensity at $\theta = 0^\circ$ when the electric field aligns along the O-C direction and to a suppression at $\theta = 180^\circ$ when the field heads in the opposite direction. Meanwhile, when the electric field is perpendicular to the molecular axis, the effect is almost insignificant. The phenomenon is thought to be linked to the ionization process. However, this picture is not completed yet. By solving the TDSE within the SAE approximation and conducting a classical simulation, we are able to obtain the ionization probability as well as the ionization rate and prove that HHG, in fact, receives a major contribution from electrons ionized at only a certain time interval, rather than throughout the whole pulse propagation. Including DCeP, the variation of the ionization rate in this interval highly correlates to that of the HHG intensity. To better demonstrate the origin of this manifestation, we also show the alternation DCeP makes on the effective potential that corresponds to the observed change in the ionization rate and consequently the HHG intensity. Our results confirm previous studies' observations and, more importantly, provide the missing physical explanation. With the role of DCeP now better understood for the entire range of the orientation angle, this effect can be handled more conveniently for calculating the HHG of other targets.

DOI: 10.1103/PhysRevA.97.043405

I. INTRODUCTION

High-order harmonic generation (HHG) is an interesting nonlinear optical phenomenon when atoms or molecules interact with an intense ultrashort laser field [1,2]. HHG spectra, ranging up to the soft x-ray regime [3–6], can provide a source of attosecond [7–10] and zeptosecond pulses [11,12] have become a powerful tool to probe and control molecular dynamics [13–19].

Ab initio calculations of high-order harmonic as well as other strong field processes by directly solving the time-dependent Schrödinger equation (TDSE) give very good references for comparison with experimental data. There are studies using *ab initio* methods to investigate HHG and ionization processes for simple molecules such as H_2^+, HeH^{2+} [20–24], and H_2 [25–28]. However, these methods are not practical for more-than-two-electron systems. In this case, it is more common for methods based on the single-active-electron (SAE) approximation [2,29–35]. There are two other widely used approximate methods, namely the time-dependent density functional theory (TDDFT) [36,37] and the multiconfiguration time-dependent Hartree-Fock (MCTDHF) methods [38,39]. But these methods do have their own disadvantages. The former is expensive with regard to computational cost. The latter, while in general saving a little in computational resources with including the correlation effect into the core, lacks an exact formulation for the exchange-correlation potential. Therefore, in our investigation, we choose the TDSE method within the SAE approximation, which is more economic than the two previously mentioned.

Due to the nature of the SAE approximation, its validity can only be assessed by comparison with experiments or full calculations done with the TDDFT or MCTDHF methods. It is shown that the SAE approximation applicability depends on the systems and on parameters of laser pulses [31,40–42]. For instance, the multielectron effects in harmonic processes have been shown to be significant for CO_2 and N_2 [15,43,44], but in the latter study [41] using the TDDFT, there exists a threshold of laser intensity for which the SAE approximation is still valid. A similar investigation for the O_2 molecule leads to the same conclusion [45]. For a larger extension of multielectron effects for both homonuclear (N_2 and F_2) and heteronuclear diatomic molecules (CO, BF, and HF), see Ref. [42]. In the same work, it is concluded that with low laser intensity, HHG spectra from all the heteronuclear molecules are mainly contributed by the highest occupied molecular orbital (HOMO). Therefore, the TDSE method incorporated with the SAE approximation may be a valuable approach for investigating multielectron systems, such as those found in Refs. [29,30,35,46–48].

In recent years, besides symmetric molecules, researchers have also been interested in asymmetric ones such as HeH^{2+}, CO, or OCS polar molecules, whose interactions with ul-

*lethicamtu@tdt.edu.vn
†hoanglv@hcmue.edu.vn

trashort lasers have led to several fascinating effects due to the role of multielectron molecular structures [24,49–54]. Particularly, Zhang *et al.* [51,52] have investigated the influence of dynamic core-electron polarization (DCeP) on the ionization and high-order harmonic processes of CO molecules by using the TDHF method. The ionization probability was calculated by the TDHF method based on the single-active orbital approximation (SAO) and was compared to the full TDHF results [51]. It has been shown that inclusion of core-electron polarization in calculations, i.e., SAO + P, improves significantly the quality of calculations based on the SAO and results in better agreement of the theoretical ionization probability with experimental data. This is also confirmed in the work of Hoang *et al.* [47] by the TDSE + SAE method. For harmonic processes, by using the TDHF method, Zhang *et al.* [51] pointed out that the SAO + P method can reproduce the main feature of HHG that the SAO cannot. In addition, they also discovered that HHG intensity changes when adding DCeP to the calculations, and besides, enhancement or suppression of HHG intensity is up to the molecular orientation in the laser field, namely parallel or antiparallel. The role of DCeP in HHG intensity enhancement or suppression of polar molecules is meaningful and needs to be thoroughly investigated.

To explain the mechanism of how DCeP affects HHG intensity, the ionization probability as a function of molecular orientation needs to be analyzed. Zhang *et al.* [51] mentioned the role of ionization but did not explain in detail. Therefore, in this work, we investigate the influence of DCeP on high-order harmonic generation of CO molecules as a function of molecular orientation by the TDSE + SAE method, i.e., solving the TDSE within the framework of the SAE approximation with and without considering DCeP. Then, by studying the ionization and kinetic energy of electrons returning to the parent ion as a function of time, we can explain completely the change in CO's harmonic intensity as a function of molecular orientation. The ionization rate is calculated by the TDSE + SAE method too. The paper is organized as follows. In Sec. II, we present the theoretical methods used for calculating ionization and harmonic spectra for linear molecules. Section III presents results, analysis, and discussion. We finish the paper with a summary in Sec. IV. Unless otherwise stated, atomic units are used throughout this paper.

II. THEORETICAL METHODS

Within the SAE approximation, we need to solve the time-dependent Schrödinger equation

$$i\frac{\partial}{\partial t}\Psi(\mathbf{r},t) = \hat{H}\Psi(\mathbf{r},t), \tag{1}$$

where $\Psi(\mathbf{r},t)$ is the wave function of the active electron. The Hamiltonian of a linear molecule subjected to a linear laser is given by

$$\hat{H} = \hat{H}_0 + V(\mathbf{r},t). \tag{2}$$

Here, $\hat{H}_0 = -\frac{1}{2}\nabla^2 + V_{\rm SAE}(\mathbf{r})$ is the field-free Hamiltonian, and $V(\mathbf{r},t) = V_{\rm L}(\mathbf{r},t) + V_{\rm P}(\mathbf{r},t)$ is the interaction potential. $V_{\rm SAE}(\mathbf{r})$ is the single-active-electron potential of a linear molecule including electrostatic (electron-nuclear attraction and electron-electron repulsion) and electron exchange potentials. The construction is described in Refs. [32,33]. The electron exchange potential is evaluated within the local density approximation (LDA) and the gradient correction term to the SAE potential has a Coulomb asymptotic behavior as in the LBα model [55]. We can choose the parameters (α,β) of the LBα model to obtain the correct ionization potential. In this work, we construct the SAE potential by one iteration with $\alpha = 1.15$ and $\beta = 0.05$ and obtain the 5σ energy of -0.52 a.u. consistently with the experimental value of -0.514 a.u. The initial potential is constructed using the wave functions from the GAUSSIAN 03 package [56]. In the length gauge, the interaction between the active electron and the laser electric field $\mathbf{E}(t)$ is given by

$$V_{\rm L}(\mathbf{r},t) = \mathbf{E}(t)\cdot\mathbf{r}. \tag{3}$$

To study the influence of dynamic core-electron polarization due to the laser field, as in Ref. [51] we add the polarization potential

$$V_{\rm P}(\mathbf{r},t) = -\frac{\mathbf{E}(t)\hat{\alpha}_{\rm c}\mathbf{r}}{r^3}. \tag{4}$$

Here, $\hat{\alpha}_{\rm c}$ is the total polarizability tensor of the core electrons whose values for CO molecules are given in Ref. [47].

The time-dependent Schrödinger equation, whose Hamiltonian is given in Eq. (2) with or without $V_{\rm P}(\mathbf{r},t)$, can be solved by the TDSE + SAE method described in Ref. [57]. We fix the nuclei at the experimental equilibrium distance during time propagation. The time-dependent wave functions are expressed as a linear combination of eigenfunctions of the field-free Hamiltonian $\hat{H}_0$. Therefore, to construct the basis set for solving the TDSE, we solve the time-independent Schrödinger equation taking into account the molecular symmetry. The wave functions Φ_n^m are expanded in the B-spline basis set B_j^k [58] multiplied by spherical harmonics Y_l^m as follows:

$$\Phi_n^m(\mathbf{r}) = \sum_{j=1}^{N_r}\sum_{l=0}^{l_{\rm max}} c_{jl}^n \frac{B_j^k(r)}{r} Y_l^m(\vartheta,\varphi), \tag{5}$$

where N_r is the number of B-spline functions and k is the order of B_j^k, in this work we choose $k = 9$. The set of eigenvalues and eigenfunctions of the field-free Hamiltonian $\hat{H}_0$ can be obtained by solving the generalized eigenvalue problem, for more details refer to Refs. [33,58]. Then, we use one of the orbitals occupied in the initial state, which is the HOMO in this case, as an active one together with all initially unoccupied orbitals as the basis set for the time-dependent wave function

$$\Psi(\mathbf{r},t) = \sum_{m=-\infty}^{\infty}\sum_{n=1}^{\infty} C_n^m(t)\Phi_n^m(\mathbf{r}), \tag{6}$$

where $C_n^m(t)$ are time-dependent coefficients. In practice, the infinity series needs to be truncated. In this work, we find that the results are convergent with the expansion of m from -20 to 20. The series of n can be controlled by the value of energy of states Φ_n^m. In our calculations, we expand to the states with energy of about 6 a.u. (about $13.6U_p$, here U_p is the ponderomotive energy and is defined later).

Plugging Eq. (6) into the Schrödinger equation (1) and then multiplying from the left with $\Phi_n^{m*}(\mathbf{r})$, after integrating over coordinates $\mathbf{r}$, we have the coupled set of ordinary first-order

differential equations:

$$i\frac{d}{dt}C_n^m(t) = E_n^m C_n^m(t) + \sum_{n',m'} \left\langle \Phi_n^m(\mathbf{r}) \middle| V(\mathbf{r},t) \middle| \Phi_{n'}^{m'}(\mathbf{r}) \right\rangle C_{n'}^{m'}(t). \quad (7)$$

In Eq. (7), the coefficients $C_n^m(t)$ are obtained by the fourth-order Runge-Kutta method. The size of the computational box $R_{\max}$ is predicted from the classical picture, where this value should be greater than the classical trajectory of an electron in the electric field $r_q = E_{\max}/\omega_0^2$. To avoid the reflection of the wave packet from the boundary, we apply a $\cos^{1/8}$ mask function [59] in the range $[r_{\text{mask}}, R_{\max}]$. Our calculations with the box size are at least three times larger than r_q, while r_{mask} starting from about $2R_{\max}/3$ can reproduce the main features of HHG spectra. However, the box size should be big enough for the mask function not to perturb the physical system, in other words, the box size needs to be bigger than $3r_q$ so that the obtained results are insensitive to the value of r_{mask}. In this work, we use $R_{\max} = 80$ a.u. and $r_{\text{mask}} = 70$ a.u.; other parameters are $N_r = 150$ and $l_{\max} = 50$. The total number of basis sets used for the time propagation is about 142 000 with the time step of 0.055 a.u. All parameters have been checked to make sure that the results are convergent in a few percent error.

With the time-dependent wave functions obtained, the ionization probability is calculated by subtracting the probability at the bound states (the survival probability) as

$$P_i(t) = 1 - \sum_{\substack{n,m \\ E_n^m < 0}} \left| \left\langle \Phi_n^m(\mathbf{r}) \middle| \Psi(\mathbf{r},t) \right\rangle \right|^2. \quad (8)$$

We can obtain HHG spectra by calculating the dipole acceleration [60] and transforming it into the frequency domain through Fourier transformation:

$$S(\omega) \propto \left| \int_0^\tau \frac{d^2}{dt^2} \langle \mathbf{r}(t) \rangle e^{-i\omega t} dt \right|^2, \quad (9)$$

where τ is the pulse duration of a laser field and $\langle \mathbf{r}(t) \rangle = \langle \Psi(\mathbf{r},t) | \mathbf{r} | \Psi(\mathbf{r},t) \rangle$ is the dipole moment of the molecule. In our further analysis considering the role of DCeP, both parallel and perpendicular components of harmonic spectra with respect to laser polarization, in general, exhibit the same behavior. Therefore, for illustrative purposes, we only show results regarding the parallel component. Readers should infer that our stated conclusions also hold for the perpendicular part.

III. RESULTS AND DISCUSSION

The linear laser used in this work has three optical cycles, $\tau = 3T$, with a wavelength of 800 nm and the electric field given as $E(t) = E_{\max} \sin^2(\frac{\pi t}{\tau}) \sin(\omega_0 t + \phi_{\text{CEP}})$. Here, $E_{\max}$ is the peak of the field amplitude, ω_0 is the laser frequency, and ϕ_{CEP} is the carrier envelope phase (CEP). Assume that the laser is linearly polarized in the yz plane and the CO molecule is aligned along the z axis with the C atom located at the positive part and the O atom located at the negative part. The internuclear separation is fixed at the experimental value of 2.132 a.u. The laser makes an orientation angle θ with the molecular axis: $\theta = 0^\circ$ when the electric field at time t_1 (defined below) points from O to C, and $\theta = 180^\circ$ when $\mathbf{E}(t_1)$ points from C to O.

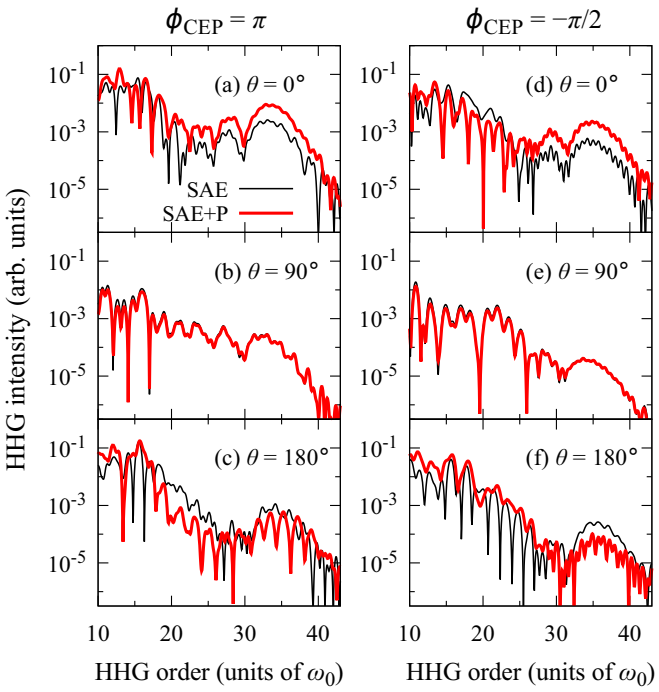

FIG. 1. HHG spectra from the CO molecule for $\theta = 0^\circ$, 90°, and 180° obtained within the SAE approximation with and without DCeP for $\phi_{\text{CEP}} = \pi$ [panels (a)–(c)] and $\phi_{\text{CEP}} = -\pi/2$ [panels (d)–(f)]. Notice that in both cases of CEP, the spectral shift caused by DCeP is upward for $\theta = 0^\circ$, downward for $\theta = 180^\circ$, and negligible for $\theta = 90^\circ$.

A. High-harmonic spectra from CO

First, we present the harmonic spectra from CO by solving the time-dependent Schrödinger equation within the framework of the SAE approximation. Figures 1(a)–1(f) show HHG spectra for the laser with $E_{\max} = 0.0755$ a.u. in two cases of the carrier envelop phase ϕ_{CEP}, namely $\phi_{\text{CEP}} = \pi$ and $\phi_{\text{CEP}} = -\pi/2$. The cutoffs of HHG spectra at about 34th order for $\phi_{\text{CEP}} = \pi$ and about 36th order for $\phi_{\text{CEP}} = -\pi/2$ are in good agreement with the formula $\omega_{\text{cutoff}} = 1.32I_p + E_{\text{kin}}$ [2], where I_p is the ionization potential and E_{kin} is the maximum kinetic energy acquired by the free electron from the laser field. Specifically, according to our classical simulation $E_{\text{kin}} \approx 2.89U_p$ for $\phi_{\text{CEP}} = \pi$, and $E_{\text{kin}} \approx 3.17U_p$ for $\phi_{\text{CEP}} = -\pi/2$, in which the ponderomotive energy $U_p = E_{\max}^2/4\omega_0^2$. It should be noted that the abovementioned formula for cutoff was derived for the case $I_p \ll U_p$ only. For $I_p/U_p = 1.17$ as in our case the more accurate calculations based on the theory given in Ref. [2] lead to the formula $\omega_{\text{cutoff}} = 1.28I_p + E_{\text{kin}}$; however it does not affect our conclusions.

Another noticeable feature in these HHG spectra is a strong orientation effect: for $\theta = 180^\circ$, the HHG spectra have pronounced minima at about 27th order for $\phi_{\text{CEP}} = \pi$ and at about 31st for $\phi_{\text{CEP}} = -\pi/2$ due to the laser-deformed orbital as discussed in Refs. [52,61]; while for $\theta = 0^\circ$, there are no

such minima. Based on these facts, the quality of our obtained HHG spectra from the SAE-TDSE for CO is reliable for further analysis.

B. Influence of dynamic core-electron polarization on harmonic spectra from CO

In this subsection, we study the influence of dynamic core-electron polarization on the HHG spectra of CO not only for $\theta = 0^\circ$ and 180° but also for the entire range of molecular orientation angles. Regardless of CEP, with the inclusion of the polarization potential $V_P(\mathbf{r},t)$ in the calculations, named SAE + P, the harmonic intensity near cutoff is increased for $\theta = 0^\circ$ [see Fig. 1(a)] and decreased for $\theta = 180^\circ$ [see Fig. 1(c)]. When further studying the dependence of HHG intensity on the molecular orientation angles, we see that for θ from 0° to 90° intensities of HHGs within the SAE + P are increased, and they are decreased for θ from 90° to 180°. Especially, around $\theta = 90^\circ$ HHGs within the SAE and the SAE + P are almost the same.

These results confirm the work of Zhang *et al.* [52]. The authors suggested a scenario in which core-electron polarization affects ionization rates and consequently HHG intensity. We now test this proposal in detail. We first calculate the total ionization probabilities at the time when the laser is turned off, i.e., at $t = \tau$ for two cases: with and without considering the DCeP. However, the dependence of the ionization probability at $t = \tau$ on the orientation angles in two cases of CEP as shown in Fig. 2 does not support the observed enhancement or suppression in HHG spectra. Indeed, if HHG correlates to the total ionization probability, then from Fig. 2(a), where $\phi_{\rm CEP} = \pi$, one may conclude that HHG when DCeP is added should exhibit the strongest enhancement at $\theta = 0^\circ$ or $\theta = 180^\circ$ and suppression for $60^\circ < \theta < 120^\circ$; while for $\phi_{\rm CEP} = -\pi/2$ as shown in Fig. 2(b), a downward shift in parallel configuration and an upward shift in antiparallel configuration are expected. In both cases, the inferred behavior is not consistent with the observed one in HHG intensity. Moreover, the change in total ionization in the presence of DCeP is sensitive to CEP, at least in the cases of $\phi_{\rm CEP} = \pi$ and $\phi_{\rm CEP} = -\pi/2$, but the response in HHG spectra to the inclusion of DCeP as shown in Fig. 1 in these two cases does not alter in general. These contradictions show that the total ionization is not a satisfactory explanation for the core effect on HHG. The next section is devoted to resolving this dilemma based on classical simulation.

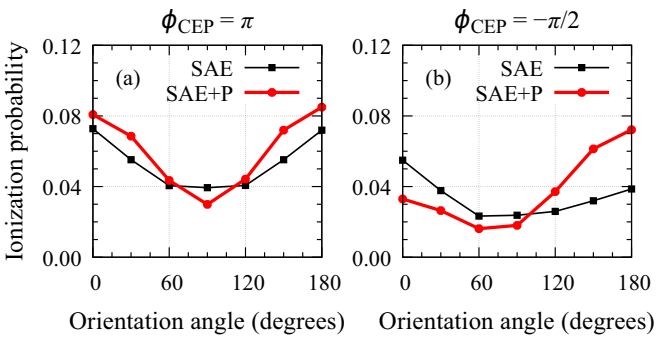

FIG. 2. The total ionization probability as a function of molecular orientation angles calculated by Eq. (8) at $t = \tau$ for two cases: (a) $\phi_{\rm CEP} = \pi$ and (b) $\phi_{\rm CEP} = -\pi/2$. The DCeP effect on total ionization strongly depends on the carrier envelop phase, which is different from what is observed in the HHG intensity.

C. Explanation

As previously mentioned, the effect of DCeP on HHG cannot be explained if one assumes the correlation between total ionization and HHG yield. Hence, to estimate how ionization throughout laser propagation contributes to HHG spectra, we use the classical model of a particle electron driven by a laser electric field with the assumption that the electron appears in the continuum energy region at the ionization time t_i at the origin with zero velocity, i.e., $z(t_i) = 0$ and $\dot{z}(t_i) = 0$. This electron is driven in the continuum region by the laser electric field only and the Coulomb interaction with the nuclei is neglected. Therefore, the electron motion is given by Newton's second law $-E(t) = \ddot{z}$. At the returning time t_r satisfying $z(t_r) = 0$, we can calculate the kinetic energy of the returning electron by the formula $E_{\rm kin} = \dot{z}^2(t_r)/2$. This energy is then converted to a HHG photon through the relation $\omega = 1.28I_p + E_{\rm kin}$.

Figure 3 shows the kinetic energy of returning electrons at the moment of recombination with the parent ion as a function of ionization time. It is clearly seen from Figs. 3(a) and 3(b) for the case of $\phi_{\rm CEP} = \pi$ that the electron ionized at around $t_1 = 1.25T$ gains the kinetic energy $E_{\rm kin} \approx 3\,U_p$ and can emit photons with frequency corresponding to the cutoff order. The electron ionized at around and after $t_2 = 1.75T$ just dominates in the low-energy region of harmonic spectra. Notice that electron can also gain $E_{\rm kin} \approx 3\,U_p$ at around the moment $t = 0.75T$; however, the ionization probability (as well as the

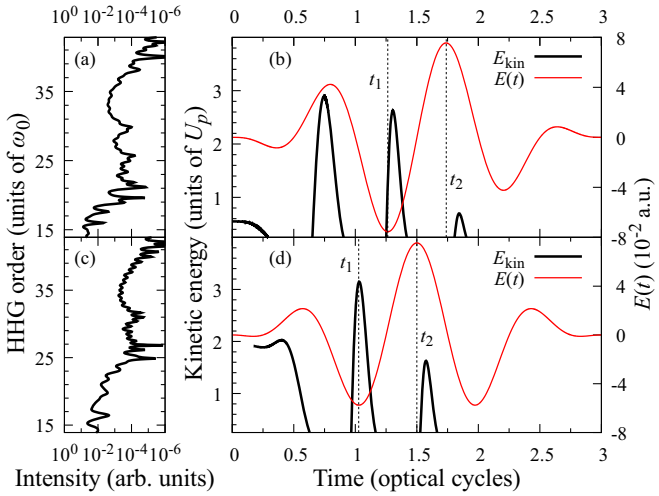

FIG. 3. Kinetic energy of the electrons returning to the parent ion CO as a function of the ionization time. The laser electric field is given as an indication of time; a HHG spectrum from CO molecules is given vertically as reference for the kinetic energy. For the case of $\phi_{\rm CEP} = \pi$, panels (a) and (b) show that electrons ionized at $t = 0.75T$ or $t_1 = 1.25T$ of the laser period have returning energy capable of emitting photons corresponding to the cutoff order; electrons ionized at the second peak just compose the low-energy part of the spectra. Similarly, in panels (c) and (d) for the case of $\phi_{\rm CEP} = -\pi/2$ the near-cutoff region originates from ionization around $t_1 = T$.

ionization rate) at this subpeak is so small that its contribution can be ignored. Similarly, Figs. 3(c) and 3(d) for the case of $\phi_{\rm CEP} = -\pi/2$ show that the electron ionized at $t_1 = T$ contributes to the high energy of harmonic spectra. From this classical picture, we can see that the near-cutoff region where DCeP manifests most strongly is mostly contributed from electrons ionized around t_1.

Having pinpointed the ionization time that contributes to HHG cutoff, we next study the time-dependent ionization rate of the CO molecule calculated with and without DCeP, focusing in the region between the two consecutive peaks t_1 and t_2. The time-dependent ionization rate is defined as

$$\Gamma(t) = -\frac{d[\ln P_{\rm b}(t)]}{dt},$$

where $P_{\rm b}(t)$ is the time-dependent survival probability [62], in which the wave functions are obtained by the TDSE + SAE method (with and without including the core-electron polarization potential). Now, as illustrated in Fig. 4, the mechanism of the DCeP effect on HHG becomes obvious. For both cases $\phi_{\rm CEP} = \pi$ and $-\pi/2$, comparing the SAE + P with the SAE, the ionization rate around t_1 is raised when $\theta = 0^\circ$, lowered when $\theta = 180^\circ$, and mostly intact when $\theta = 90^\circ$. This perfectly matches the effect of DCeP on HHG intensity. Note that the ionization rate around t_2 is not consistent with that around t_1, but as shown previously, the electron ionized at this time only makes up the lower-energy part of the spectra and thus is irrelevant to our argument.

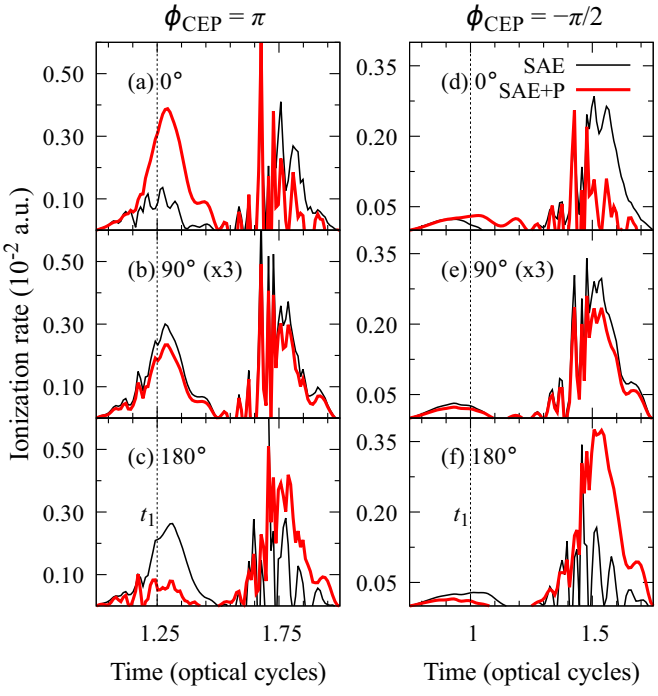

FIG. 4. The time-dependent ionization rate of the CO molecule calculated with and without DCeP: left panels, (a)–(c), for $\phi_{\rm CEP} = \pi$; and right panels, (d)–(f), for $\phi_{\rm CEP} = -\pi/2$. The figure shows that the ionization rate is high at the peak(s) of intensity of the laser pulse. This means that the total ionization yield is mainly contributed by the ionization at the peak(s). By including the DCeP in the calculations, the ionization rate around the moment t_1 increases or decreases depending on the molecular orientation in consistency with the changing of the HHG intensity given in Fig. 1.

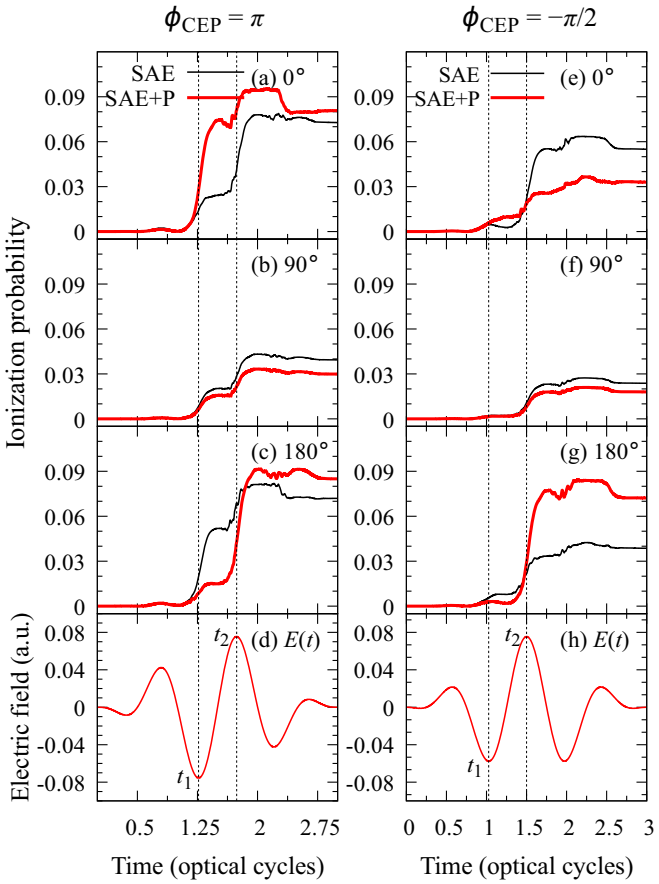

FIG. 5. The time-dependent ionization probability of the CO molecule for $\theta = 0^\circ$, 90°, and 180° calculated with or without DCeP: left panels, (a)–(d), for $\phi_{\rm CEP} = \pi$; and right panels, (d)–(h), for $\phi_{\rm CEP} = -\pi/2$. For illustration, the electric fields of laser pulses are also given. The vertical lines mark the effective time period from $t_1 = 1.25T$ to $t_2 = 1.75T$ for $\phi_{\rm CEP} = \pi$ and from $t_1 = T$ to $t_2 = 1.5T$ for $\phi_{\rm CEP} = -\pi/2$. By including DCeP into the calculations (TDSE + SAE + P), the time-dependent ionization probability at the moment in this effective period is increased or decreased and corresponds to the enhancement or suppression of the HHG intensity given in Fig. 1.

For other visual illustration, we also show the time-dependent ionization probability for two investigated CEPs and three orientation angles. From Fig. 4, in the period around t_1 until before t_2, the ionization rate is highest around t_1. Therefore, the ionization probability in the period $[t_1, t_2]$ is dominated by ionization at t_1. Figure 5 shows the time-dependent ionization probability of CO molecule for $\theta = 0^\circ$, 90°, and 180° calculated with or without DCeP for two cases of the carrier envelop phase of laser electric field $\phi_{\rm CEP} = \pi$ and $\phi_{\rm CEP} = -\pi/2$. For illustration of various moments of ionization, the electric fields of laser pulses are also given in the figures. With including the DCeP into calculations, the time-dependent ionization probability at the moment in the effective period is increased or decreased in the correlation to the enhancement or suppression of the HHG intensity given in Fig. 1.

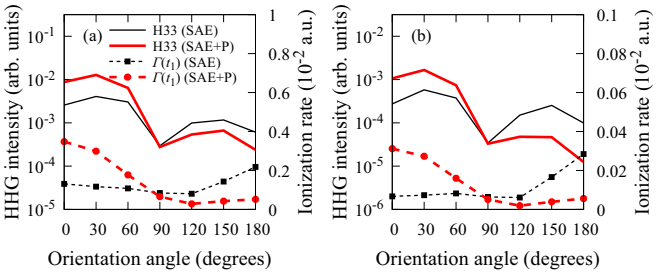

FIG. 6. The ionization rate at t_1 and the harmonic intensity of 33rd order as functions of orientation angle for two cases: (a) $\phi_{CEP} = \pi$ and (b) $\phi_{CEP} = -\pi/2$. In both cases of CEP, the harmonic intensities within the SAE + P are greater than those within the SAE for the molecular orientation angle $\theta < 90^\circ$ and, in contrast, are smaller for $\theta > 90^\circ$. Around $\theta = 90^\circ$ the harmonic intensity within the SAE + P is nearly equal to that of within the SAE. It is clearly seen that the variation of the ionization rate at t_1 by including DCeP as a function of the molecular orientation angle is the same as the variation of the harmonic intensity.

Further illustration of the DCeP effect on HHG intensity can be seen also in Fig. 6, which shows both the HHG intensity of 33rd order and the ionization rate at t_1 as functions of the molecular orientation angle. One can see that the variation of the ionization rate at t_1 by including DCeP as a function of the molecular orientation angle is the same as the variation of the harmonic intensity. This illustration together with the previous ones fully support the idea that HHG cutoff is mostly composed of electrons ionized around t_1 and DCeP affects HHG spectra via ionization rate at this point in time.

The variation of ionization probability around t_1 is due to the distortion on potential by the laser. In Fig. 7 we visualize the effective potential including the SAE potential V_{SAE} and the interaction potential for two cases: with and without the polarization potential V_P at $t_1 = T$ by the laser with $\phi_{CEP} = -\pi/2$. The potential is plotted along the z axis for the orientation $\theta = 0^\circ$ and $\theta = 180^\circ$, but for the orientation $\theta = 90^\circ$ the z component of the potential is not affected by the laser field so the potential is plotted along the y axis instead. For the case of $\phi_{CEP} = \pi$ the figures are similar and are not presented here. During time propagation, we calculate the

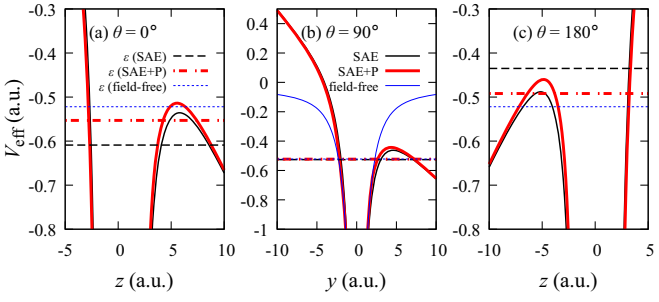

FIG. 7. Effective potential along the z axis at $t_1 = T$ for $\theta = 0^\circ$ (a) and $\theta = 180^\circ$ (c) and along the y axis for $\theta = 90^\circ$ (b). The horizontal lines are the orbital energies 5σ in field-free (short dashed blue line) and field-dressed: SAE (dashed black line) and SAE + P (dot-dashed red line). The data are for the laser with $\phi_{CEP} = -\pi/2$; for the case of $\phi_{CEP} = \pi$ the figures are similar.

expected energy value of the 5σ orbital ε (for the SAE + P and the SAE) corresponding to with and without V_P and plot them in the same figures. It should be noted that the idea of using the effective potential for demonstration of the DCeP effect on ionization was first introduced in Ref. [51].

Figure 7 shows that the barrier potential including V_P is higher for both orientations $\theta = 0^\circ$ and 180°. However, the field-dressed orbital energy with DCeP ε (SAE + P) is shifted more than ε (SAE) for $\theta = 0^\circ$ and less than ε (SAE) for $\theta = 180^\circ$. For $\theta = 90^\circ$, the effective potentials are almost unchanged by including V_P, and, consequently, the energy ε (SAE) is equal to ε (SAE + P). As a result, the gap between the potential barrier height and the orbital energy is narrowed when $\theta = 0^\circ$, intact when $\theta = 90^\circ$, and widened when $\theta = 180^\circ$. Hence, we have completely explained the mechanism that allows the core-electron polarization effect on HHG near-cutoff intensity to depend strongly on orientation angles but not carrier envelop phases.

IV. CONCLUSION

In this work, we present the HHG spectra from CO molecules calculated by the TDSE+SAE method, i.e., solving the time-dependent Schrödinger equation within the SAE approximation. We confirm the DCeP effect on harmonic intensity, introduced first in Ref. [52] for the molecular orientations of $\theta = 0^\circ$ and $\theta = 180^\circ$ by the TDHF method. The DCeP effect is further investigated for the entire range of the molecular orientation angle θ from 0° to 180°. We see that the DCeP shift is positive for $\theta = 0^\circ$ to near 90° when HHG intensities within the SAE + P are increased in comparison with that by the SAE. In contrast, the DCeP shift is negative for θ from near 90° to 180°.

With the laser used in this work, the results indicate that the harmonic intensity is dominated by the highest occupied molecular orbital, still consistent with the results of Ref. [42]. Moreover, by investigating the time-dependent ionization probability as well as the time-dependent ionization rate, we explain completely the DCeP effect on harmonic intensity based on two statements: (i) the main contribution to the HHG intensity is only the ionization around the moment t_1 of the laser pulse; (ii) including the core-electron polarization potential in the calculations (SAE + P) leads to the variation (increase or decrease) of the ionization rate at this time, which, in turn, results in the similar variation of the HHG intensity.

The specified value of t_1 is roughly the subpeak of laser pulse that electrons ionized at which can recombine with the parent ion and emit photons with the frequency corresponding to the cutoff order. Thanks to the time-dependent ionization rate around this time, one can predict the influence of dynamic core-electron polarization on the harmonic intensity, at least for CO molecules. Now, we understand why the DCeP effect for HHG intensity is not sensitive to the CEP of laser field although this effect for the total ionization yields is strongly dependent on CEP. An extension of study for other linear molecules would be also interesting.

ACKNOWLEDGMENTS

This research is funded by the Vietnam National Foundation for Science and Technology Development (NAFOS-

TED) under Grant No. 103.01-2017.371. V.H.H. is supported by the Program of Fundamental Research of Ministry of Education and Training (Vietnam) under Grant No. B2016.19.10. This work is carried out thanks to the HPC cluster at Ho Chi Minh City University of Education, Vietnam.

[1] A. McPherson, G. Gibson, H. Jara, U. Johann, T. S. Luk, I. A. McIntyre, K. Boyer, and C. K. Rhodes, J. Opt. Soc. Am. B **4**, 595 (1987).
[2] M. Lewenstein, P. Balcou, M. Y. Ivanov, A. L'Huillier, and P. B. Corkum, Phys. Rev. A **49**, 2117 (1994).
[3] J. Seres, E. Seres, A. J. Verhoef, G. Tempea, C. Streli, P. Wobrauschek, V. Yakovlev, A. Scrinzi, C. Spielmann, and F. Krausz, Nature (London) **433**, 596 (2005).
[4] T. Popmintchev, M.-C. Chen, A. Bahabad, M. Gerrity, P. Sidorenko, O. Cohen, I. P. Christov, M. M. Murnane, and H. C. Kapteyn, Proc. Natl. Acad. Sci. U.S.A. **106**, 10516 (2009).
[5] C. Jin, G. J. Stein, K.-H. Hong, and C. D. Lin, Phys. Rev. Lett. **115**, 043901 (2015).
[6] G. J. Stein, P. D. Keathley, P. Krogen, H. Liang, J. P. Siqueira, C.-L. Chang, C.-J. Lai, K.-H. Hong, G. M. Laurent, and F. X. Kärtner, J. Phys. B: At. Mol. Opt. Phys. **49**, 155601 (2016).
[7] A. Scrinzi, M. Y. Ivanov, R. Kienberger, and D. M. Villeneuve, J. Phys. B: At. Mol. Opt. Phys. **39**, R1 (2006).
[8] P. B. Corkum and F. Krausz, Nat. Phys. **3**, 381 (2007).
[9] C. Zhang, G. Vampa, D. M. Villeneuve, and P. B. Corkum, J. Phys. B: At. Mol. Opt. Phys. **48**, 061001 (2015).
[10] L. Medišauskas, J. Wragg, H. van der Hart, and M. Y. Ivanov, Phys. Rev. Lett. **115**, 153001 (2015).
[11] C. Hernandez-Garcia, J. A. Perez-Hernandez, T. Popmintchev, M. M. Murnane, H. C. Kapteyn, A. Jaron-Becker, A. Becker, and L. Plaja, Phys. Rev. Lett. **111**, 033002 (2013).
[12] D. J. Dunning, B. W. McNeil, and N. R. Thompson, Phys. Procedia **52**, 62 (2014).
[13] J. Itatani, J. Levesque, D. Zeidler, H. Niikura, H. Pepin, J. C. Kieffer, P. B. Corkum, and D. M. Villeneuve, Nature (London) **432**, 867 (2004).
[14] S. Baker, J. S. Robinson, C. A. Haworth, H. Teng, R. A. Smith, C. C. Chirilă, M. Lein, J. W. G. Tisch, and J. P. Marangos, Science **312**, 424 (2006).
[15] O. Smirnova, Y. Mairesse, S. Patchkovskii, N. Dudovich, D. Villeneuve, P. Corkum, and M. Y. Ivanov, Nature (London) **460**, 972 (2009).
[16] A. D. Shiner, B. E. Schmidt, C. Trallero-Herrero, H. J. Wörner, S. Patchkovskii, P. B. Corkum, J.-C. Kieffer, F. Légaré, and D. M. Villeneuve, Nat. Phys. **7**, 464 (2011).
[17] D. Shafir, H. Soifer, B. D. Bruner, M. Dagan, Y. Mairesse, S. Patchkovskii, M. Y. Ivanov, O. Smirnova, and N. Dudovich, Nature (London) **485**, 343 (2012).
[18] C. Neidel, J. Klei, C.-H. Yang, A. Rouzée, M. J. J. Vrakking, K. Klünder, M. Miranda, C. L. Arnold, T. Fordell, A. L'Huillier, M. Gisselbrecht, P. Johnsson, M. P. Dinh, E. Suraud, P.-G. Reinhard, V. Despré, M. A. L. Marques, and F. Lépine, Phys. Rev. Lett. **111**, 033001 (2013).
[19] P. M. Kraus, B. Mignolet, D. Baykusheva, A. Rupenyan, L. Horný, E. F. Penka, G. Grassi, O. I. Tolstikhin, J. Schneider, F. Jensen, L. B. Madsen, A. D. Bandrauk, F. Remacle, and H. J. Wörner, Science **350**, 790 (2015).
[20] M. Lein, N. Hay, R. Velotta, J. P. Marangos, and P. L. Knight, Phys. Rev. Lett. **88**, 183903 (2002).
[21] G. Lagmago Kamta and A. D. Bandrauk, Phys. Rev. A **70**, 011404 (2004).
[22] K.-J. Yuan and A. D. Bandrauk, J. Phys. B: At. Mol. Opt. Phys. **45**, 074001 (2012).
[23] B. Fetić and D. B. Milošević, Phys. Rev. E **95**, 053309 (2017).
[24] G. L. Kamta, A. D. Bandrauk, and P. B. Corkum, J. Phys. B: At. Mol. Opt. Phys. **38**, L339 (2005).
[25] M. Lein and C. Chirilă, Chem. Phys. **366**, 54 (2009).
[26] M. Awasthi, V. V. Yulian, and A. Saenz, J. Phys. B: At. Mol. Opt. Phys. **38**, 3973 (2005).
[27] X. Guan, K. Bartschat, and B. I. Schneider, Phys. Rev. A **83**, 043403 (2011).
[28] W.-C. Jiang, L.-Y. Peng, J.-W. Geng, and Q. Gong, Phys. Rev. A **88**, 063408 (2013).
[29] E. Cormier and P. Lambropoulos, J. Phys. B: At. Mol. Opt. Phys. **30**, 3095 (1997).
[30] I. A. Ivanov and A. S. Kheifets, J. Phys. B: At. Mol. Opt. Phys. **42**, 145601 (2009).
[31] C. Vozzi, M. Negro, F. Calegari, G. Sansone, M. Nisoli, S. De Silvestri, and S. Stagira, Nat. Phys. **7**, 822 (2011).
[32] M. Abu-samha and L. B. Madsen, Phys. Rev. A **81**, 033416 (2010).
[33] S.-F. Zhao, C. Jin, A.-T. Le, T. F. Jiang, and C. D. Lin, Phys. Rev. A **81**, 033423 (2010).
[34] S. Petretti, Y. V. Vanne, A. Saenz, A. Castro, and P. Decleva, Phys. Rev. Lett. **104**, 223001 (2010).
[35] T.-Y. Du, Z. Guan, X.-X. Zhou, and X.-B. Bian, Phys. Rev. A **94**, 023419 (2016).
[36] M. A. L. Marques and E. K. U. Gross, Annu. Rev. Phys. Chem. **55**, 427 (2004).
[37] A. Castro, H. Appel, M. Oliveira, C. A. Rozzi, X. Andrade, F. Lorenzen, M. A. L. Marques, E. K. U. Gross, and A. Rubio, Phys. Status Solidi B **243**, 2465 (2006).
[38] J. Zanghellini, M. Kitzler, T. Brabec, and A. Scrinzi, J. Phys. B: At. Mol. Opt. Phys. **37**, 763 (2004).
[39] J. Caillat, J. Zanghellini, M. Kitzler, O. Koch, W. Kreuzer, and A. Scrinzi, Phys. Rev. A **71**, 012712 (2005).
[40] M. Awasthi and A. Saenz, Phys. Rev. A **81**, 063406 (2010).
[41] E. P. Fowe and A. D. Bandrauk, Phys. Rev. A **81**, 023411 (2010).
[42] J. Heslar, D. Telnov, and Shih-I Chu, Phys. Rev. A **83**, 043414 (2011).
[43] S. Patchkovskii, Z. Zhao, T. Brabec, and D. M. Villeneuve, Phys. Rev. Lett. **97**, 123003 (2006).
[44] B. K. McFarland, J. P. Farrell, P. H. Bucksbaum, and M. Guhr, Science **322**, 1232 (2008).
[45] J. Zhang, Y. Wu, Z. Zeng, and Z. Xu, Phys. Rev. A **88**, 033826 (2013).
[46] S.-F. Zhao, L. Liu, and X.-X. Zhou, Opt. Commun. **313**, 74 (2014).

[47] V.-H. Hoang, S.-F. Zhao, V.-H. Le, and A.-T. Le, Phys. Rev. A **95**, 023407 (2017).
[48] A. Schild and E. K. U. Gross, Phys. Rev. Lett. **118**, 163202 (2017).
[49] H. Miyagi, T. Morishita, and S. Watanabe, Phys. Rev. A **85**, 022708 (2012).
[50] H. Li, D. Ray, S. De, I. Znakovskaya, W. Cao, G. Laurent, Z. Wang, M. F. Kling, A. T. Le, and C. L. Cocke, Phys. Rev. A **84**, 043429 (2011).
[51] B. Zhang, J. Yuan, and Z. Zhao, Phys. Rev. Lett. **111**, 163001 (2013).
[52] B. Zhang, J. Yuan, and Z. Zhao, Phys. Rev. A **90**, 035402 (2014).
[53] H. Hu, N. Li, P. Liu, R. Li, and Z. Xu, Phys. Rev. Lett. **119**, 173201 (2017).
[54] L. Holmegaard, J. L. Hansen, L. Kalhoj, S. Louise Kragh, H. Stapelfeldt, F. Filsinger, J. Kupper, G. Meijer, D. Dimitrovski, M. Abu-samha, C. P. J. Martiny, and L. Bojer Madsen, Nat. Phys. **6**, 428 (2010).
[55] R. van Leeuwen and E. J. Baerends, Phys. Rev. A **49**, 2421 (1994).
[56] M. J. Frisch *et al.*, Gaussian 03, Revision C.02, Gaussian, Inc., Wallingford, CT, 2004.
[57] M. Awasthi, Y. V. Vanne, A. Saenz, A. Castro, and P. Decleva, Phys. Rev. A **77**, 063403 (2008).
[58] H. Bachau, E. Cormier, P. Decleva, J. E. Hansen, and F. Martín, Rep. Prog. Phys. **64**, 1815 (2001).
[59] H. Yu and A. D. Bandrauk, Phys. Rev. A **56**, 685 (1997).
[60] K. Burnett, V. C. Reed, J. Cooper, and P. L. Knight, Phys. Rev. A **45**, 3347 (1992).
[61] M. D. Spiewanowski, A. Etches, and L. B. Madsen, Phys. Rev. A **87**, 043424 (2013).
[62] D. A. Telnov, K. Nasiri Avanaki, and Shih-I Chu, Phys. Rev. A **90**, 043404 (2014).